HETEROGENEOUS DISTRIBUTION OF ^{26}Al AT THE BIRTH OF THE SOLAR SYSTEM

Kentaro Makide[1], Kazuhide Nagashima[1], Alexander N. Krot[1,4], Gary R. Huss[1],
Fred J. Ciesla[2], Eric Hellebrand[3], Eric Gaidos[3], and Le Yang[2]

[1] Hawai'i Institute of Geophysics and Planetology, School of Ocean, Earth Science and Technology, University of Hawai'i at Mānoa,
Honolulu, HI 96822, USA; sasha@higp.hawaii.edu
[2] Department of the Geophysical Sciences, University of Chicago, Chicago, IL 60637, USA
[3] Department of Geology and Geophysics, University of Hawai'i at Mānoa, Honolulu, HI 96822, USA

ABSTRACT

It is believed that ^{26}Al, a short-lived ($t_{1/2} = 0.73$ Ma) and now extinct radionuclide, was uniformly distributed in the nascent solar system (SS) with the initial ^{26}Al/^{27}Al ratio of $\sim 5.2 \times 10^{-5}$, suggesting an external, stellar origin rather than local, solar source. However, the stellar source of ^{26}Al and the manner in which it was injected into the SS remain controversial: the ^{26}Al could have been produced by an asymptotic giant branch star, a supernova, or a Wolf–Rayet star and injected either into the protosolar molecular cloud, protosolar cloud core, or protoplanetary disk. Corundum (Al$_2$O$_3$) is predicted to be the first condensate from a cooling gas of solar composition. Here we show that micron-sized corundum condensates from ^{16}O-rich (Δ^{17}O ~ -25‰) gas of solar composition recorded heterogeneous distribution of ^{26}Al at the birth of the SS: the inferred initial ^{26}Al/^{27}Al ratio ranges from $\sim 6.5 \times 10^{-5}$ to $<2 \times 10^{-6}$; 52% of corundum grains measured are ^{26}Al-poor. Abundant ^{26}Al-poor, ^{16}O-rich refractory objects include grossite- and hibonite-rich calcium–aluminum-rich inclusions (CAIs) in CH (high metal abundance and high iron concentration) chondrites, platy hibonite crystals in CM (Mighei-like) chondrites, and CAIs with fractionation and unidentified nuclear effects CAIs chondrites. Considering the apparently early and short duration (<0.3 Ma) of condensation of refractory ^{16}O-rich solids in the SS, we infer that ^{26}Al was injected into the collapsing protosolar molecular cloud and later homogenized in the protoplanetary disk. The apparent lack of correlation between ^{26}Al abundance and O-isotope composition of corundum grains constrains the stellar source of ^{26}Al in the SS.

Key words: meteorites, meteors, meteoroids – protoplanetary disks – stars: Wolf–Rayet – Sun: evolution – supernovae: general

Online-only material: machine-readable table

1. INTRODUCTION

^{26}Al (which decays to ^{26}Mg with a half-life, $t_{1/2} = 0.73$ Ma), ^{10}Be ($t_{1/2} = 1.5$ Ma), ^{36}Cl ($t_{1/2} = 0.3$ Ma), ^{41}Ca ($t_{1/2} = 0.1$ Ma), ^{53}Mn ($t_{1/2} = 3.7$ Ma), and ^{60}Fe ($t_{1/2} = 2.3$ Ma) are short-lived radionuclides that were present in the early solar system (SS; McKeegan & Davis 2003). The recently inferred uniform distribution of ^{26}Al in the early SS (Jacobsen et al. 2008; Villeneuve et al. 2009; Davis et al. 2010) makes the ^{26}Al–^{26}Mg system one of the most important relative chronometers of the early SS processes, such as the evaporation, condensation, and melting of solids in the protoplanetary disk (McKeegan & Davis 2003; Kita et al. 2005; Krot et al. 2009). The maximum amount of ^{26}Al that could have been produced by solar energetic particle irradiation is insufficient to explain the canonical ^{26}Al/^{27}Al ratio ($\sim 5.2 \times 10^{-5}$) and suggests a stellar, nucleosynthetic origin of ^{26}Al (Duprat & Tatischeff 2007). The stellar source of ^{26}Al and the mechanism by which it was introduced into the SS, however, remain controversial. Possible sources of freshly synthesized ^{26}Al are a neighboring asymptotic giant branch (AGB) star (Wasserburg et al. 2006), a supernova (SN; Boss et al. 2008), or a wind from a Wolf–Rayet (WR) star (Arnould et al. 2006; Gaidos et al. 2009; Tatischeff et al. 2010), any of which could have injected ^{26}Al into the parent molecular cloud (Gaidos et al. 2009), protosolar cloud core (Boss et al. 2008), or protoplanetary disk (Ouellette et al. 2007).

AGB stars are not associated with star-forming regions and the probability of an encounter between an AGB star and a star-forming molecular cloud is very low, $\sim 2.5 \times 10^{-6}$ (Huss

et al. 2009). Although massive SN progenitors are commonly associated with star-forming regions (Lada & Lada 2003), the probability of injection of ^{26}Al into the protosolar cloud core or protoplanetary disk from a nearby SN is also low, $\leqslant 3 \times 10^{-3}$ (Williams & Gaidos 2007; Gounelle & Meibom 2008). To overcome this problem, it has been recently suggested that the Sun was born in a stellar cluster of second generation that was self-enriched in short-lived radionuclides (^{60}Fe and possibly ^{26}Al) by a single or multiple 10–15 solar mass ($M_\odot$) SN several million years before our SS formed (Gounelle et al. 2009). Finally, it was proposed that ^{26}Al could have been added to the progenitor molecular cloud by WR wind (Arnould et al. 2006; Gaidos et al. 2009; Tatischeff et al. 2010).

CAIs are the oldest SS solids dated (Amelin et al. 2002; Bouvier & Wadhwa 2010) and are believed to have formed when the Sun was a class 0 or class I protostar (e.g., Krot et al. 2009; Tscharnuter et al. 2009), although Ciesla (2010) argues that most CAIs found in meteorites formed at the time that the solar nebula stopped accreting significant amounts of material from the protosolar parent cloud, and thus corresponds roughly to the class I–class II transition. The majority of CAIs in unmetamorphosed chondrites have the initial ^{26}Al/^{27}Al ratio ((^{26}Al/^{27}Al)$_0$) of $\sim (4$–5$) \times 10^{-5}$ (MacPherson et al. 1995; Jacobsen et al. 2008; Makide et al. 2009b). CAIs with low (^{26}Al/^{27}Al)$_0$, $\ll 5 \times 10^{-6}$, are very rare (Makide et al. 2009b; Sahijpal & Goswami 1998; Liu et al. 2009), except in CH chondrites where they are dominant (Krot et al. 2008). CH chondrites escaped thermal metamorphism and aqueous alteration, and are considered to be one of the most primitive meteorites in our collections. These ^{26}Al-poor CAIs are interpreted either to be the result of early formation, prior to injection and homogenization

---
[4] Author to whom any correspondence should be addressed.

of ^{26}Al in the SS (Makide et al. 2009b; Sahijpal & Goswami 1998; Liu et al. 2009; Krot et al. 2008) or as a result of preferential loss of ^{26}Al carrier from CAI precursors by sublimation (Thrane et al. 2008). The late-stage formation of ^{26}Al-poor CAIs, after decay of ^{26}Al, can also not be excluded, because CAIs are known to have experienced multistage thermal processing in the solar nebula and on chondrite parent asteroids (Krot et al. 2005) that could have erased possible evidence for radiogenic ^{26}Mg (MacPherson et al. 1995).

Corundum (Al_2O_3) is predicted to be the first condensate from a cooling gas of solar composition (Ebel & Grossman 2000). Therefore, corundum condensates can potentially provide additional constraints on the origin of ^{26}Al and degree of its heterogeneity in the nascent SS. The pioneering work on solar corundum grains was done by Virag et al. (1991), who studied 26 individual corundum grains 3–20 μm grains from the unmetamorphosed CM carbonaceous chondrite (CC) Murchison. On the basis of the oxygen and magnesium-isotopic compositions, the grains were divided into three groups. Group 1 ($n = 17$) and group 2 ($n = 5$) grains show ^{26}Mg excesses corresponding to $(^{26}Al/^{27}Al)_0$ of 5×10^{-5} and 5×10^{-6}, respectively; group 3 grains ($n = 4$) show no resolvable ^{26}Mg excesses ($(^{26}Al/^{27}Al)_0$ $<3 \times 10^{-7}$).

To understand the origin and distribution of ^{26}Al in the early SS, we measured ^{26}Al–^{26}Mg isotope systematics and oxygen-isotope compositions of micron-sized corundum grains from acid-resistant residues of unequilibrated ordinary chondrites (UOCs; H (high total iron contents) and LL (low metallic iron and low total iron contents) of low petrologic type, $\leqslant$3.15) and unmetamorphosed CCs (CI1 (Ivuna-like), CM2, CR2 (Renazzo-like), and CO3.0 (Ornans-like)) using the University of Hawai'i (UH) Cameca ims-1280 ion microprobe. Oxygen isotopes were used to distinguish solar from presolar corundum grains; the latter are characterized by isotopically anomalous oxygen compositions (Nittler 2003) compared to the solar and terrestrial values, $\Delta^{17}O \sim -25$‰ and 0‰, respectively (Makide et al. 2009b; McKeegan et al. 2010), where $\Delta^{17}O = \delta^{17}O - 0.52 \times \delta^{18}O$, $\delta^{17,18}O = ((^{17,18}O/^{16}O)_{sample}/(^{17,18}O/^{16}O)_{SMOW} - 1) \times 1000$, and SMOW is the Standard Mean Ocean Water.

2. ANALYTICAL PROCEDURES

2.1. Sample Preparation

Acid-resistant residues of ordinary and CCs used in this study were prepared by Huss & Lewis (1995) and Huss et al. (2003). The residues consist of SiC, spinel ($MgAl_2O_4$), hibonite ($CaAl_{12}O_{19}$), and corundum and range in size from 0.5 to 5 μm. The residues were diluted by a mixture of 90% isopropanol and 10% water and mixed in an ultrasonic bath. About 0.2 μl of the mixture was siphoned using a micro-aspirator and dispersed onto a gold substrate under a stereomicroscope. More than 100 grains were dispersed on each gold substrate. Prior to the dispersion, the gold substrate was examined for possible contamination using the UH JEOL JXA-8500F field emission electron microprobe (FE-EPMA) equipped with a cathodoluminescence detector (CL) and an energy dispersive spectrometer (EDS). Several relatively large (>5 μm) corundum grains embedded in the substrates were identified and avoided during subsequent oxygen- and magnesium-isotopic measurements. To locate the chondritic corundum grains comprising less than 1% of the dispersed grains dominated by spinel, we used CL and EDS of the FE-EPMA. Among the dispersed grains, only corun-

dum and SiC show intense CL; the latter is very rare and can easily be distinguished by EDS. The corundum grains identified were imaged in secondary and backscattered electrons.

2.2. Oxygen- and Magnesium-isotope Measurements

Oxygen-isotope compositions of individual corundum grains were measured with the UH Cameca ims-1280 (for details see Makide et al. 2009a).

Aluminum- and magnesium-isotope measurements with UH Cameca ims-1280 were conducted on the corundum grains which have been previously analyzed for oxygen isotopes. An ^{16}O$^-$ primary beam, either defocused ($\sim$30 μm spotsize) or focused ($\sim$3 μm), was used to generate secondary Mg$^+$ and Al$^+$ ions. A field aperture of 1000×1000 μm^2 corresponding to $\sim$7 μm on the sample was used to minimize the contribution of Mg signals from the substrate and other dispersed grains surrounding the grain of interest. The contribution of the Mg signal from the substrate was estimated to be <1% of Mg from the sample. The mass resolving power was set to $\sim$3500–3800, sufficient to separate interfering hydrides and ^{48}Ca^{++}. Secondary ions of ^{24}Mg$^+$, ^{25}Mg$^+$, and ^{26}Mg$^+$ were measured simultaneously using the monocollector electron measure (EM) and two multicollector EMs; ^{27}Al$^+$ was subsequently measured with the monocollector EM by peak-jumping. The primary beam current was adjusted so that the ^{27}Al$^+$ count rate did not exceed 4.5×10^5 cps. Acquisition times for Mg isotopes and ^{27}Al were 15 s and 1 s, respectively. Each measurement consisted of 20 cycles. Excess of radiogenic ^{26}Mg (δ^{26}Mg*) was calculated using the following equation: $\delta^{26}Mg^* = \Delta^{26}Mg - 2 \times \Delta^{25}Mg$, where $\Delta^{25,26}Mg = ((^{25,26}Mg/^{24}Mg)_{sample})/(^{25,26}Mg/^{24}Mg)_{ref} - 1) \times 1000$ and reference Mg-isotope ratios are from Catanzaro et al. (1966). We note that $\Delta^{25,26}Mg$ values wre calculated using the mean of ratios for all cycles. Since Mg count rates are low, it results in bias in $^{25}Mg/^{24}Mg$ and $^{26}Mg/^{24}Mg$ ratios (Ogliore et al. 2011). The typical reproducibility of standard measurements was $\sim$10‰ (2σ) in Δ^{25}Mg and Δ^{26}Mg. To correct for instrumental mass fractionation effects and estimate the relative sensitivity factor for the $^{27}Al/^{24}Mg$ ratio, we used a Montana sapphire (α-Al_2O_3) standard (NMNH 126321 from the Smithsonian Institution). The instrumental fractionation correction was made based on the measurements of micron-sized Montana sapphire grains dispersed on the gold substrate. To correct the $^{27}Al^+/^{24}Mg^+$ ratios measured by SIMS in micron-sized corundum grains, we measured the Mg concentration in the Montana sapphire grain by the UH FE-EPMA; a piece of the same grain was also measured by multicollector inductively coupled plasma mass spectrometry (MC-ICPMS) by E. D. Young (UCLA). To measure trace amount of Mg in the sapphire by FE-EPMA, we used defocused (10 μm) electron beam at $\sim$300 nA current and 15 keV accelerating voltage. Madagascar hibonite was used as a standard. The $^{27}Al/^{24}Mg$ ratios in the sapphire obtained by FE-EPMA and LA MC-ICP-MS are 6084 ± 498 (2σ, 45 spots) and 5830 ± 510 (2σ, 4 spots), respectively, and are the same within the uncertainties and show no evidence for heterogeneity.

3. RESULTS AND DISCUSSION

3.1. Oxygen- and Magnesium-isotope Compositions of Micron-sized Corundum Grains

Oxygen-isotope compositions of micron-sized corundum grains from acid-resistant residues of UOCs (Semarkona (LL3.0), Bishunpur (LL3.1), Roosevelt County (RC) 075 (H3.1)) and unmetamorphosed CCs (Orgueil (CI1),

Table 1
Oxygen-isotope Compositions (in ‰) and the Inferred $(^{26}Al/^{27}Al)_0$ Ratios from Individual Micron-sized Corundum Grain in UOCs and Unmetamorphosed CCs

Grain	$\delta^{18}O$	2σ	$\delta^{17}O$	2σ	$\Delta^{17}O$	2σ	$(^{26}Al/^{27}Al)_0 \times 10^{-5}$	2σ
Carbonaceous chondrites								
ALHA 03-03	−35.9	2.3	−43.4	4.5	−24.7	4.7	N.D.	
. . .								

Notes.

Sem, Semarkona; Bis, Bishunpur; RC075, Roosevelt County 075; ALHA, Alan Hills A77307; Murr, Murray; Org, Orgueil; Ren, Renazzo; *P, presolar grains; *U, isotopically unusual grains, possibly an analytical artifact. The *P and *U grains are not plotted in Figure 1. N.D. = not determined. ˆgrains with O-isotope compositions reported by Makide et al. (2009a).

(This table is available in its entirety in a machine-readable form in the online journal. A portion is shown here for guidance regarding its form and content.)
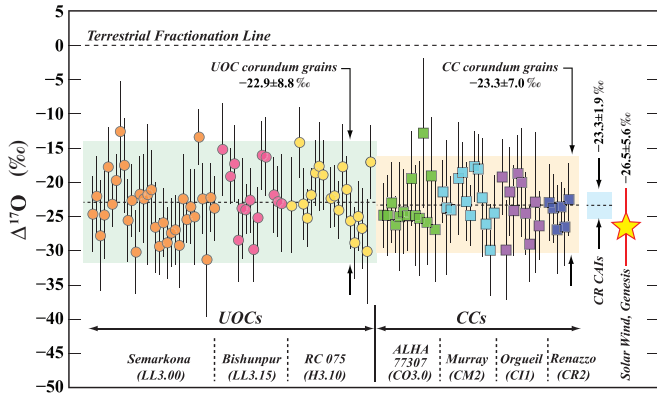
Figure 1. $\Delta^{17}O$ values of micron-sized corundum grains from unequilibrated ordinary chondrites (UOCs) and unmetamorphosed carbonaceous chondrites (CCs), CAIs from CR chondrites (Makide et al. 2009b), and solar wind (McKeegan et al. 2010). Errors are 2σ. The ^{16}O-rich composition of corundum grains similar to those of CR CAIs and solar wind is consistent with a condensation origin from a gas of solar composition. Petrologic types of ordinary chondrites are from Grossman & Brearley (2005).

Murray (CM2), Renazzo (CR2), and Allan Hills (ALH) A77307 (CO3.0)) together with compositions of the mineralogically pristine CAIs from CR2 CCs (Makide et al. 2009b) and the solar wind returned by the Genesis spacecraft (McKeegan et al. 2010) are listed in online Table 1 and plotted in Figure 1. All but three corundum grains have ^{16}O-rich compositions similar to those of CR CAIs and solar wind, consistent with a condensation origin from an ^{16}O-rich gas of solar composition. Three corundum grains, not shown in Figure 1, have highly anomalous O-isotope compositions, and are probably presolar in origin.

The solar corundum grains were subsequently measured for magnesium-isotope compositions and $^{27}Al/^{24}Mg$ ratio; the results are listed in Table 1 and plotted in Figure 2. The grains show large variations of the inferred initial $^{26}Al/^{27}Al$ ratio $((^{26}Al/^{27}Al)_0)$: 52% of grains have no resolvable $^{26}Mg*$: an upper limit on $(^{26}Al/^{27}Al)_0$ is 2×10^{-6}; 40% of grains have high $(^{26}Al/^{27}Al)_0$, $(3.0–6.5) \times 10^{-5}$; 8% of grains have intermediate values of $(^{26}Al/^{27}Al)_0$, $(1–2) \times 10^{-5}$.

The coexistence of the ^{26}Al-rich and ^{26}Al-poor corundum grains in the same primitive meteorite precludes late-stage (after decay of ^{26}Al) resetting of the ^{26}Al–^{26}Mg systematics of the ^{26}Al-poor corundum grains during thermal metamorphism in the host chondrite parent body. Late-stage resetting in the solar nebula during thermal processing associated with chondrule formation is also excluded. Chondrule formation occurred in an ^{16}O-poor ($\Delta^{17}O > -10‰$) nebular reservoir (e.g., Krot et al.

2006) when ^{26}Al was still alive (Kita et al. 2005; Kurahashi et al. 2008; Krot et al. 2009). We infer that ^{16}O-rich corundum grains with low initial $^{26}Al/^{27}Al$ ratios never contained the canonical abundance of ^{26}Al, i.e., the lack of ^{26}Mg excess in 52% of ^{16}O-rich corundum grains is a primary characteristic.

### 3.2. Multiple Generations of CAIs and Refractory Grains and Their Distribution in the Protoplanetary Disk

A high abundance ($>50\%$) of ^{26}Al-poor, ^{16}O-rich CAIs has been previously reported in CH CCs (Krot et al. 2006). Similar to corundum grains, the CH CAIs are among the smallest ($<20\ \mu m$) and the most refractory (rich in hibonite and grossite, $CaAl_4O_7$) objects known (Krot et al. 2002). The ^{26}Al heterogeneity and high abundance of ^{26}Al-poor, ^{16}O-rich refractory objects in a fine fraction of solar dust can be explained in the context of the formation setting of refractory objects (MacPherson et al. 1995; Krot et al. 2009) and theoretical modeling of their radial transport in the protoplanetary disk (Boss 2008; Ciesla 2009, 2010; Yang & Ciesla 2010). Refractory objects are thought to have formed in region(s) with high ambient temperature (at or above condensation temperature of forsterite (Mg_2SiO_4), ~ 1350 K at total pressure of $<10^{-4}$ bar), most likely within 1–2 astronomical units from the Sun (Krot et al. 2009, and references therein). They were subsequently transported outward to the accretion regions of chondrite parent asteroids and cometary nuclei (Gounelle & Meibom 2007; Boss 2008; Ciesla 2009, 2010). The oldest ^{207}Pb–^{206}Pb absolute ages of CAIs from CV (Vigaranolike) chondrites (Amelin et al. 2002; Bouvier & Wadhwa 2010), a narrow range of their initial $^{26}Al/^{27}Al$ ratios (Jacobsen et al. 2008), corresponding to a range of crystallization ages of <0.1 Ma, and the high ambient temperature in the CAI-forming region(s), are all consistent with an early and brief duration of CAI formation, during a period of high mass-accretion rate of dust and gas to the proto-Sun ($\sim 10^{-6}\ M_\odot\ yr^{-1}$; Krot et al. 2009; Ciesla 2009). We propose that the ^{26}Al-poor and ^{26}Al-rich ^{16}O-rich corundum grains represent different generations of refractory objects formed during a brief epoch of CAI formation, and, therefore, reflect heterogeneous or variable ^{26}Al at the birth of the SS.

To understand the distribution of refractory objects with the different $(^{26}Al/^{27}Al)_0$ in the early SS, we modeled the evolution of a viscous disk and redistribution of refractory objects formed in the high-temperature (above 1400 K) region within it during the first million years of its evolution (Figure 3). We consider both the mass and angular momentum transport in the disk as well as the addition of mass to both the Sun and the disk due to infall from the parent molecular cloud (Yang & Ciesla
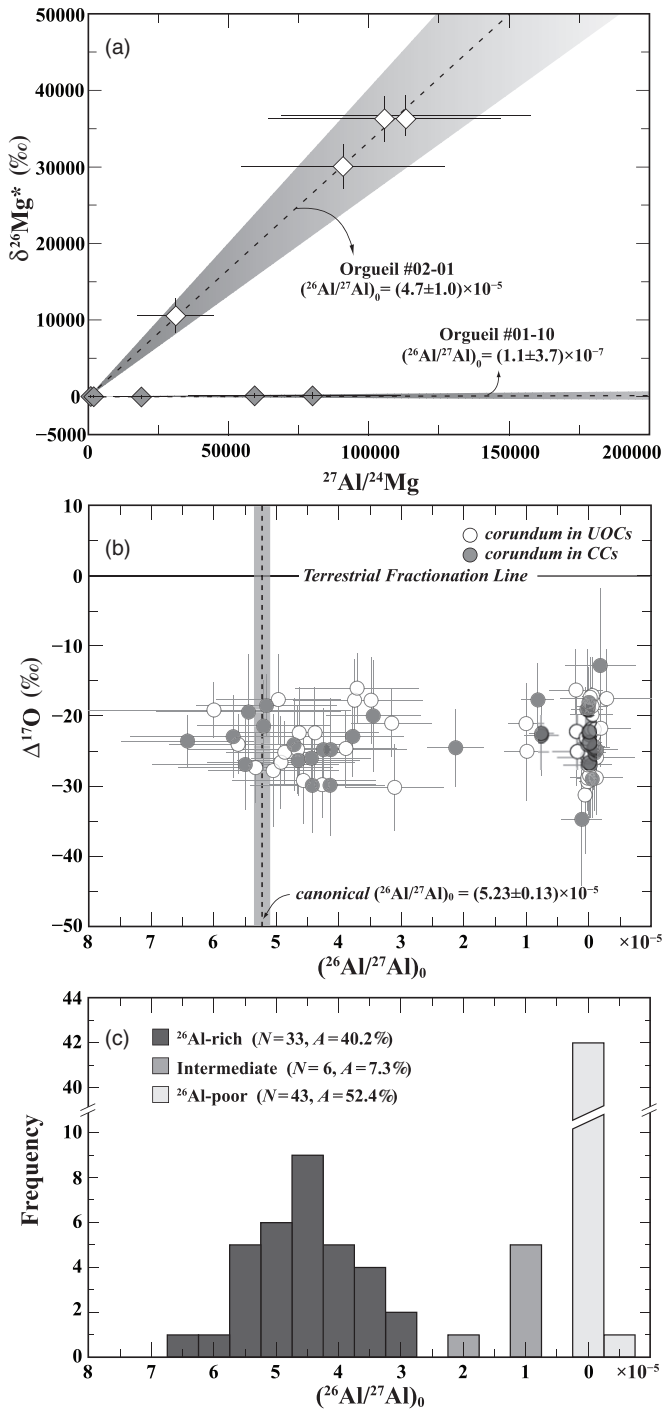
Figure 2. (a) Aluminum–magnesium evolutionary isotope diagram for the micron-sized corundum grains #02–01 and #01–10 from Orgueil. The grain #02–01 has excesses of ^{26}Mg corresponding to the initial ^{26}Al/^{27}Al ratio ((^{26}Al/^{27}Al)$_0$) of $(4.7 \pm 1.0) \times 10^{-5}$. No resolvable excess of ^{26}Mg is found in the grain #01–10; an upper limit on (^{26}Al/^{27}Al)$_0$ is 4.8×10^{-7}. Errors are 2σ. (b) Δ^{17}O values vs. (^{26}Al/^{27}Al)$_0$ in corundum grains from UOCs and CCs. Errors are 2σ. There is a bi-modal distribution of (^{26}Al/^{27}Al)$_0$: 52% of grains have no detectable excess of ^{26}Mg (an upper limit on (^{26}Al/^{27}Al)$_0$ is 2×10^{-6}); 40% of grains have large excesses of ^{26}Mg corresponding to (^{26}Al/^{27}Al)$_0$ from $\sim 3.0 \times 10^{-5}$ to $\sim 6.5 \times 10^{-5}$; 8% of grains have intermediate values of (^{26}Al/^{27}Al)$_0$. There is no correlation between O- and ^{26}Al–^{26}Mg systematics of corundum grains. In contrast to the corundum grains, the (^{26}Al/^{27}Al)$_0$ in whole-rock CV CAIs shows small variations, $(5.23 \pm 0.13) \times 10^{-5}$. (c) The distribution of (^{26}Al/^{27}Al)$_0$ in solar corundum grains.

2010; Hueso & Guillot 2005). The parent cloud is assumed to be 1 $M_\odot$, spherical, at a temperature of 15 K, rotating with a
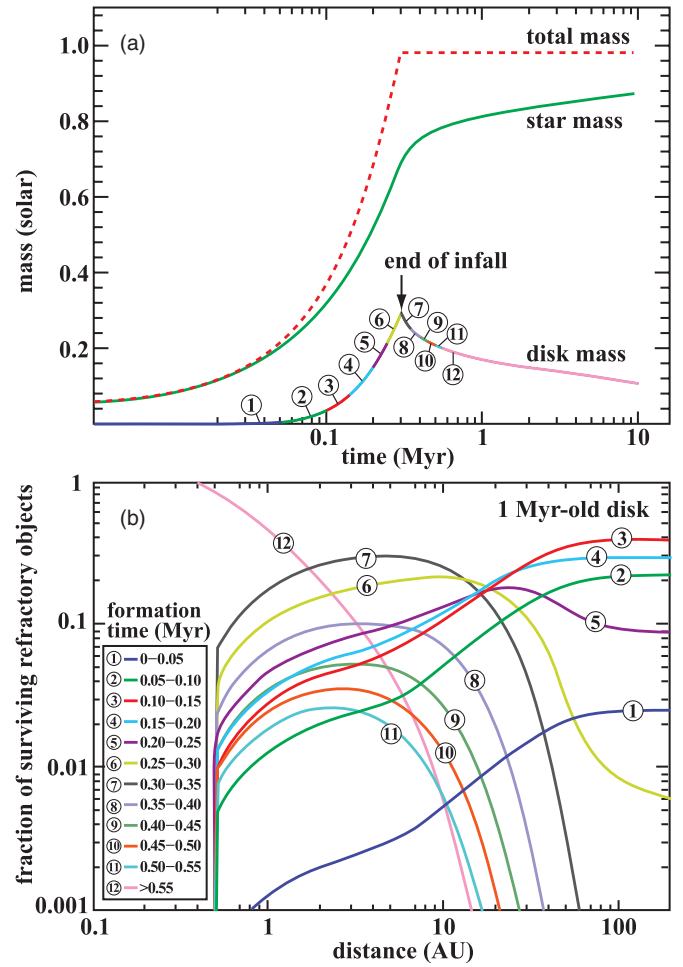
Figure 3 (a) Masses of the solar mass star, disk, and star + disk as a function of time. (b) Fraction of dust processed at high temperature (> 1400 K) and survived in a 1 Myr old disk, plotted in different batches (numbered from 1 to 12) according to when they were last exposed to those high temperatures.

uniform angular velocity of $\Omega_c = 10^{-14}$ s^{-1}, and we adopt a mass accretion rate of $\sim 3 \times 10^{-6}$ $M_\odot$ yr^{-1}; the disk viscosity is parameterized with a turbulent viscosity coefficient of $\alpha = 10^{-3}$. The accreted mass falls onto the disk at locations where the specific angular momentum in the disk equals that in the parent cloud (Yang & Ciesla 2010; Hueso & Guillot 2005). We track populations of fine refractory objects as they are redistributed throughout the disk by viscous expansion, dividing them into batches depending on the timing of when they are last exposed to the high-temperature region (Figures 3(a) and (b)).

We find that the mass of the disk reaches its maximum by 300,000 years of its evolution (Figure 3(a)), and that the most dominant population of refractory objects in a 1 million year old disk consists of those that formed immediately before and after cessation of infall from the parent molecular cloud (Figure 3(b)). This prediction, combined with the observed heterogeneity of (^{26}Al/^{27}Al)$_0$, suggests that ^{26}Al was introduced into the SS contemporaneously with the collapse of the protosolar cloud core; injection into the disk (Ouellette et al. 2007) is much less likely. Alternatively, if ^{26}Al was heterogeneously distributed in the parent molecular cloud, mixing in the disk did not homogenize it until the infall and formation of refractory solids had ceased. Thus, refractory objects formed prior to the end of collapse would not record the average solar nebula ^{26}Al/^{27}Al ratio, but rather the ratio that existed in the hot nebular region

at the time of their formation. This would allow refractory objects with different initial ^{26}Al/^{27}Al ratios (^{26}Al-poor and ^{26}Al-rich) to form and to be preserved in the disk. It also implies that the initial ^{26}Al/^{27}Al ratio of $(5.23 \pm 0.13) \times 10^{-5}$ recorded by CV CAIs (Jacobsen et al. 2008; Davis et al. 2010) may not necessarily represent the initial ^{26}Al/^{27}Al ratio in the SS.

Our modeling indicates that a significant population of refractory objects that formed prior to the cessation of infall survives in the disk (Figure 3(b)). The survival time of dust particles (up to ~1 m in size) in the disk is inversely proportional to their sizes: fine (5 μm) dust is well-coupled to the nebular gas and less affected by head wind than the coarse (~1 mm) dust (Ciesla 2010). These observations may explain the high proportion of ^{26}Al-poor refractory objects in a fine fraction of solar dust, e.g., as we have observed in corundum grains and CH CAIs, as well as the presence of an ^{26}Al-poor, ^{16}O-rich CAI in comet Wild2 (Matzel et al. 2010).

3.3. Stellar Source of ^{26}Al

The heterogeneous distribution of ^{26}Al at the birth of the SS may preclude inheritance of ^{26}Al from a molecular cloud enriched by a previous generation of stars (Gounelle et al. 2009), which is expected to have a uniform distribution of ^{26}Al. Instead, it indicates injection of ^{26}Al nearly contemporaneously with the collapse molecular cloud core that formed the SS. The similar oxygen-isotope compositions of the ^{26}Al-rich and ^{26}Al-poor corundum grains and the Sun suggest injection of ^{26}Al by a massive ($>$20 $M_\odot$) Type II SN, by a wind from a WR star or by a low-mass (1.5 $M_\odot$) AGB star (Sahijpal & Soni 2006; Krot et al. 2008; Ellinger et al. 2010). Injection of ^{26}Al by a less massive SN or by a 3–6 $M_\odot$ AGB star is unlikely, because it is expected to produce significant change in oxygen-isotope composition of the SS that has not been observed (Sahijpal & Soni 2006; Gounelle & Meibom 2007; Ellinger et al. 2010).

To distinguish between an explosive SN and a WR wind of ^{26}Al, measurements of other isotopes (e.g., ^{60}Fe–^{60}Ni isotope systematics) of ^{26}Al-rich and ^{26}Al-poor ^{16}O-rich CAIs or refractory grains are required: in contrast to SNe, the WR stars do not produce ^{60}Fe (Sahijpal & Soni 2006). Therefore, if ^{26}Al was injected by a WR star (Gaidos et al. 2009; Tatischeff et al. 2010) and ^{60}Fe was inherited from a molecular cloud of an earlier generation (Gounelle et al. 2009), the two isotopes would be decoupled, i.e., the ^{26}Al-rich and ^{26}Al-poor CAIs will have similar initial abundance of ^{60}Fe. In contrast, if ^{26}Al and ^{60}Fe were injected by the same SN, the ^{26}Al-poor CAIs would have lower initial abundance of ^{60}Fe than the ^{26}Al-rich CAIs.

We note that the initial abundance of ^{60}Fe in the SS remains controversial. The inferred initial ^{60}Fe/^{56}Fe ratios range from $(2–5) \times 10^{-7}$ (Telus et al. 2011) to $<1 \times 10^{-8}$ (Tang & Dauphas 2011). Due to the presence of nucleosynthetic isotopic anomalies in Ni, the detection of radiogenic ^{60}Ni in bulk CAIs is difficult (Quitté et al. 2007) and may require high-precision Fe–Ni isotope measurements of CAI mineral separates to construct an internal Fe–Ni isochron.

REFERENCES

Amelin, Y., Krot, A. N., Hutcheon, I. D., & Ulyanov, A. A. 2002, Science, 297, 1678
Arnould, M., Paulus, G., & Meynet, G. 2006, A&A, 321, 653
Boss, A. P. 2008, Earth Planet. Sci. Lett., 268, 102
Boss, A. P., Ipatov, S. I., Keiser, S. A., Myhill, E. A., & Vanhala, H. A. T. 2008, ApJ, 686, L119
Bouvier, A., & Wadhwa, M. 2010, Nat. Geosci., 3, 637
Catanzaro, E. J., Murphy, T. J., Garner, E. L., & Shields, W. R. 1966, J. Res. Natl Bur. Stand., 70A, 453
Ciesla, F. J. 2009, Icarus, 200, 655
Ciesla, F. J. 2010, Icarus, 208, 455
Davis, A. M., Kita, N. T., Ushikubo, T., MacPherson, G. J., Bullock, E. S., & Knight, K. B. 2010, Lunar Planet. Sci., 41, 2496
Duprat, J., & Tatischeff, V. 2007, ApJ, 671, L69
Ebel, D., & Grossman, L. 2000, Geochim. Cosmochim. Acta, 64, 339
Ellinger, C. I., Young, P. A., & Desch, S. J. 2010, ApJ, 725, 1495
Gaidos, E., Krot, A. N., Williams, J. P., & Raymond, S. N. 2009, ApJ, 696, 1854

Gounelle, M., & Meibom, A. 2007, ApJ, 664, L123
Gounelle, M., & Meibom, A. 2008, ApJ, 680, 781
Gounelle, M., Meibom, A., Hennebelle, P., & Inutsuka, S. 2009, ApJ, 694, L1
Grossman, J. N., & Brearley, A. J. 2005, Meteorit. Planet. Sci., 40, 87
Hueso, R., & Guillot, T. 2005, A&A, 442, 703
Huss, G. R., & Lewis, R. S. 1995, Geochim. Cosmochim. Acta, 59, 115
Huss, G. R., Meshik, A. P., Smith, J. B., & Hohenberg, C. M. 2003, Geochim. Cosmochim. Acta, 67, 4823
Huss, G. R., Meyer, B. S., Srinivasan, G., Gopalan, J. N., & Sahijpal, S. 2009, Geochim. Cosmochim. Acta, 73, 4922
Jacobsen, B., Yin, Q.-Z., Moynier, F., Amelin, Y., Krot, A. N., Nagashima, K., Hutcheon, I. D., & Palme, H. 2008, Earth Planet. Sci. Lett., 272, 353
Kita, N. T., Huss, G. R., Tachibana, S., Amelin, Y., Nyquist, L. E., & Hutcheon, I. D. 2005, in ASP Conf. Ser., 341, Chondrules and the Protoplanetary Disk, ed. A. N. Krot, E. R. D. Scott, & B. Reipurth (San Francisco, CA: ASP), 558
Krot, A. N., Meibom, A., Weisberg, M. K., & Keil, K. 2002, Meteorit. Planet. Sci., 37, 1451
Krot, A. N., Nagashima, K., Bizzarro, M., Huss, G. R., Davis, A. M., McKeegan, K. D., Meyer, B. S., & Ulyanov, A. A. 2008, ApJ, 672, 713
Krot, A. N., Yurimoto, H., Hutcheon, I. D., & MacPherson, G. J. 2005, Nature, 434, 998
Krot, A. N., et al. 2006, Chem. Erde, 66, 249
Krot, A. N., et al. 2009, Geochim. Cosmochim. Acta, 73, 4963
Kurahashi, E., Kita, N. T., Nagahara, H., & Morishita, Y. 2008, Geochim. Cosmochim. Acta, 72, 3865
Lada, C. J., & Lada, L. E. 2003, ARA&A, 41, 57
Liu, M.-C., McKeegan, K. D., Goswami, J. N., Marhas, K. K., Sahijpal, S., Ireland, T. R., & Davis, A. M. 2009, Geochim. Cosmochim. Acta, 73, 5051
MacPherson, G. J., Davis, A. M., & Zinner, E. K. 1995, Meteoritics, 30, 365
Makide, K., Nagashima, K., Krot, A. N., & Huss, G. R. 2009a, ApJ, 706, 142
Makide, K., Nagashima, K., Krot, A. N., Huss, G. R., Hutcheon, I. D., & Bischoff, A. 2009b, Geochim. Cosmochim. Acta, 73, 5018
Matzel, J. E. P., et al. 2010, Science, 328, 483
McKeegan, K. D., & Davis, A. M. 2003, in Treatise on Geochemistry 1, ed. A. M. Davis (Amsterdam: Elsevier), 431
McKeegan, K. D., et al. 2010, Lunar Planet. Sci., 41, 2589
Nittler, L. P. 2003, Earth Planet. Sci. Lett., 209, 259
Ogliore, R. C., Huss, G. R., & Nagashima, K. 2011, Nucl. Inst. Methods in Phys. Res. B, in press
Ouellette, N., Desch, S. J., & Hester, J. J. 2007, ApJ, 662, 1268
Quitté, G., Halliday, A. N., Meyer, B. S., Markowski, A., Latkoczy, C., & Günther, D. 2007, ApJ, 655, 678
Sahijpal, S., & Goswami, J. 1998, ApJ, 509, L137
Sahijpal, S., & Soni, P. 2006, Meteorit. Planet. Sci., 41, 953
Tang, H., & Dauphas, N. 2011, Lunar Planet. Sci., 42, 1068
Tatischeff, V., Duprat, J., & Séréville, N. 2010, ApJ, 714, L26
Telus, M., Huss, G. R., Nagashima, K., Ogliore, R. C., Tachibana, S., & Jilly, C. E. 2011, Lunar Planet. Sci., 42, 2559
Thrane, K., Nagashima, K., Krot, A. N., & Bizzarro, M. 2008, ApJ, 680, L141
Tscharnuter, W. M., Schönke, J., Gail, H.-P., Trieloff, M., & Lüttjohann, E. 2009, A&A, 504, 109
Villeneuve, J., Chaussidon, M., & Libourel, G. 2009, Science, 325, 985
Virag, A., Zinner, E., Amari, S., & Anders, E. 1991, Geochim. Cosmochim. Acta, 55, 2045
Wasserburg, G. J., Busso, M., Gallino, R., & Nollett, K. M. 2006, Nucl. Phys. A, 777, 5
Williams, J. P., & Gaidos, E. 2007, ApJ, 663, L33
Yang, L., & Ciesla, F. J. 2010, Lunar Planet. Sci., 41, 1461